

# COMPARISON ON THE SUPERCONDUCTING PROPERTIES OF Nb AND NbTiN THIN FILMS PRODUCED BY BOTH HiPIMS AND BIPOLAR HiPIMS \*

S. Simon<sup>1,2†</sup>, C. Benjamin<sup>2,3</sup>, R. Valizadeh<sup>2,3</sup>, J. W. Bradley<sup>1,2</sup>

<sup>1</sup>Department of Electrical Engineering and Electronics, University of Liverpool,  
Liverpool, United Kingdom

<sup>2</sup>Cockcroft Institute of Accelerator Science, Daresbury, United Kingdom

<sup>3</sup>STFC ASTeC, Daresbury, Warrington, United Kingdom

## Abstract

Most superconducting thin films found on SRF cavity are generally produced through magnetron sputtering using niobium (Nb) as target. Yet, this technique can still be improved as the resulting film lack in efficiency. Alternative materials such as NbTiN could potentially be used with significant improvement compared to pure Nb films. Here, we report the use of both high-power impulse magnetron (HiPIMS) and bipolar HiPIMS to produce superconducting thin films, with a particular attention on the optimal conditions to enhance the film growth highly dependent on the pressure and power conditions. We used both mass spectroscopy and optical emission spectroscopy to analyze the plasma chemistry providing information on the mass/energy of the ions formed.

## INTRODUCTION

Superconducting RF (SRF) cavities are mainly done using bulk niobium (Nb) as material due to its critical temperature ( $T_c = 9.2$  K) and critical magnetic field ( $H_c$ ) [1]. Even though Nb appears to be the material of choice compared to other pure metals, the community investigates other alternatives to reduce both production and operational costs. As most superconducting phenomenon are mainly restrain within few micrometers of the material, research is focusing on the production and improvement of superconducting material thin films on copper substrate [2],[3]. Niobium titanium nitride (NbTiN) appears to be a promising candidate for this purpose with its high critical temperature ( $T_c = 17$  K) and relatively low residual surface resistance [4].

Thin films are usually produced using physical vapour deposition such as DC magnetron sputtering (DCMS) [5] or arc evaporation [6]. High Power Impulse Magnetron Sputtering (HiPIMS) is another technique which has gathered more and more interest over the last decades for its potential to improve the quality of the thin films compared to DCMS [7]. HiPIMS allows to reach very high dense plasmas with high level of ionized species exhibiting high ion energy distribution functions (IEDF) compared to those observed in DCMS [8]. To further control the growth process, a secondary positive

pulse could be applied after the initial negative pulse known as bipolar HiPIMS. This technique can enhance the film properties due to the energetic bombardement of ions also, depending on the magnitude of the reversed potential ( $U_{rev}$ ) adhesion, density and microstructures of the deposited film can be tailored [9]. Lastly, it was reported that this process could promote the deposition rate arguing that the return effect observed in HiPIMS is reduced due to the application of the positive pulse [10].

In this work, HiPIMS and bipolar HiPIMS were investigated for the production of Nb and NbTiN thin films. In order to investigate the plasma phase, both mass- and energy-scans were recorded.

## EXPERIMENTAL PROCEDURE

The experiment were carried in a ultra high vacuum (UHV) system with a cylindrical magnetically balanced magnetron, with a base pressure of  $1 \times 10^{-8}$  mbar. For the analysis of Nb, the magnetron consisted of a cylindrical Nb rod (99.999% purity) used as sputtering material. The chamber was filled with a 20 sccm Kr flow rate (BOC, 99.999% purity) reaching a working pressure of  $1 \times 10^{-2}$  mbar. Figure 1 illustrate the discharge obtained in such conditions.

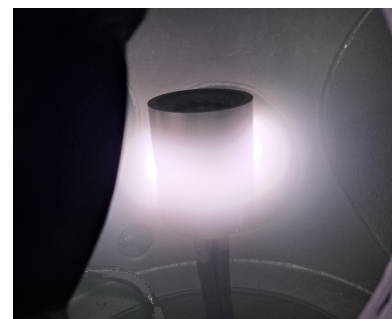


Figure 1: Picture of the discharge achieved in the chamber.

For the analysis of NbTiN, the Nb cylinder was covered by a titanium wire (1 mm diameter, 99.98% purity). The working gas was premixed (20 sccm of Kr and 2 sccm of  $N_2$  (BOC, 99.997% purity) before introduction in the chamber. The pressure of the chamber was maintained at  $1 \times 10^{-2}$  mbar using a diaphragm valve at the inlet of the turbo pump. The cathode was connected to a pulsing unit (HiPSTER 1, Ionautics AB) fed by two DC power supply. The first power

\* This work has been supported by: the I.FAST collaboration which has received funding from the European Union's Horizon 2020 Research and Innovation programme under Grant Agreement No 101004730.

† stephane.simon@liverpool.ac.uk

supply delivers a negative potential initiating classical HiPIMS pulses where the second one delivers a reverse positive potential  $U_{rev}$  varied from 0 to 50 V. The pulsing unit controlled by computer at a frequency of 1000 Hz with negative pulses of 100  $\mu$ s (duty cycle of 10%), followed by a 200  $\mu$ s positive pulse (delay of 1.5  $\mu$ s).

*In-situ* mass- and energy-dependent analyses of the positive ions were carried using a mass spectrometer (EQP-9 system, Hiden Analytical) allowing the measurements of ion energies up to 100 eV. The spectrometer was placed facing the discharge at a distance of 9 cm.

## RESULTS AND DISCUSSIONS

Figure 2 reports the mass scan obtained for the positive ions in HiPIMS where Nb was used as sputtering materials.

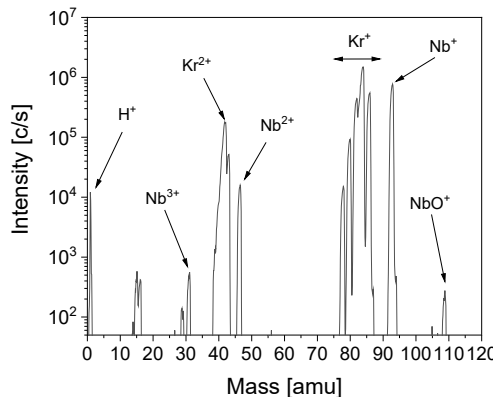


Figure 2: Mass scan for the positive ions obtained using HiPIMS and with a Nb target.

From the figure, we observed the main peaks for the single charged ions of Nb (93 amu) and Kr (78, 80, 82, 84 and 86 amu). Additionally, the second charges ions of Nb and Kr are also observed at respectively 46 and 42 amu, with  $\text{Kr}^{2+}$  having a slightly higher intensity possibly due by the return of Nb ions to the target ionising Kr atoms in the vicinity. Finally, two other ions are also detected at respectively 28 and 31 amu. These two ions could be the triple charged ions of Kr and Nb (respectively), with the possibility of 28 amu being shared with  $\text{CO}^+$ . A peak at 109 amu is also observed which could be linked to the recombination between Nb ions and free oxygen produced by the dissociation of water molecules.

Figure 3 reports the mass scan of the positive ions for a NbTi target in HiPIMS using a mixture of nitrogen and krypton as working gas. Due to gas mixture, nitrogen ions are observed at  $m/z = 28$  and 14 amu. Similarly to Fig. 2, Nb and Kr positive ions are observed at  $m/z = 93$  amu for  $\text{Nb}^+$  and  $m/z = 78, 80, 82, 84$ , and 86 amu for  $\text{Kr}^+$ ; the double charged are also observed at respectively  $m/z = 46$  and 42 amu. Regarding the triple charged ions of Nb and Kr, they seemed to be drastically reduced by the addition of nitrogen as no peak was find at  $m/z = 31$  amu for  $\text{Nb}^{+3}$ . Titanium ions

are found at  $m/z = 46, 47, 49, 50$  amu, with the dominant peak found at  $m/z = 48$  amu. This peak is also confirmed by the presence of a peak at  $m/z = 24$  amu corresponding to  $\text{Ti}^{2+}$ . Lastly, two other peaks are also observed at  $m/z = 62$  amu and  $m/z = 107$  amu. These peaks correspond to the recombination between metal ions and nitrogen ions, with the former being  $\text{TiN}^+$  and the latest  $\text{NbN}^+$ .

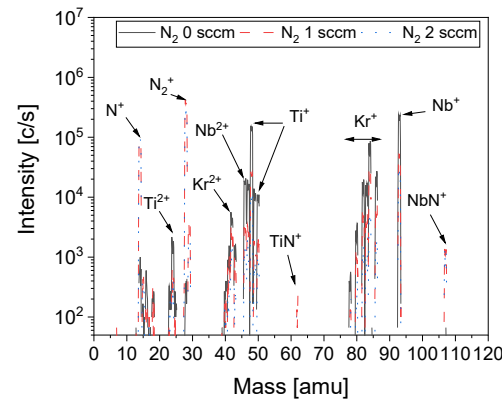


Figure 3: Mass scan of the positive ions obtained using HiPIMS with a Nb/Ti target.

The flow rate of nitrogen was varied from 0 to 2 sccm, this increase has directly an impact of the metal ions intensity (i.e., Nb and Ti) as well as the peak intensity of Kr. However, the increase benefit the peak at 62 amu ( $\text{TiN}^+$ ) and 107 amu ( $\text{NbN}^+$ ). This could be explained by the fact that the nitrogen ions are getting ionised and more available to recombined with the sputtered materials.

When looking at the bipolar HiPIMS scenario, the mass scan remain unchanged meaning their is no other formation/recombination occurring. Figure 4 reports the IEDF of the ions  $\text{Nb}^+$  (a),  $\text{Ti}^+$  (b),  $\text{Kr}^+$  (c),  $\text{N}_2^+$  and  $\text{N}^+$  (d). Starting with Fig. 4 (a), the continuous line correspond of a classic HiPIMS scenario. The peak energy reaches a maximum at around 3 eV followed by a high-energy tail. Similar trend were reported in [11] and [12]. The next curve corresponds to the use of bipolar HiPIMS with  $U_{rev}$  set at either 25 V. In this situation, a new peak appears at an energy slightly above  $eU_{rev}$ , the peak is then followed by a high-energy tail similar to what was observed in classic HiPIMS. Similar observation can be done with  $\text{Ti}^+$  reported in Fig. 4 (b). For both ions, the ion intensity of the first peak falls and does not seem to be affected by  $U_{rev}$ .

Regarding the Kr ions (Fig. 4, (c)), these follow a similar pattern as Nb and Ti positive ions. Yet, they present a more pronounced fall after the second maximum peak. From the figure and similar work reported in [13], the differences between Nb and Kr could be explained by the spatial of the ions distribution during the HiPIMS discharge. During the HiPIMS discharge, Nb atoms are sputtered from the target and ionized in its vicinity with a large fraction being attracted back to the target. These ions are then influenced

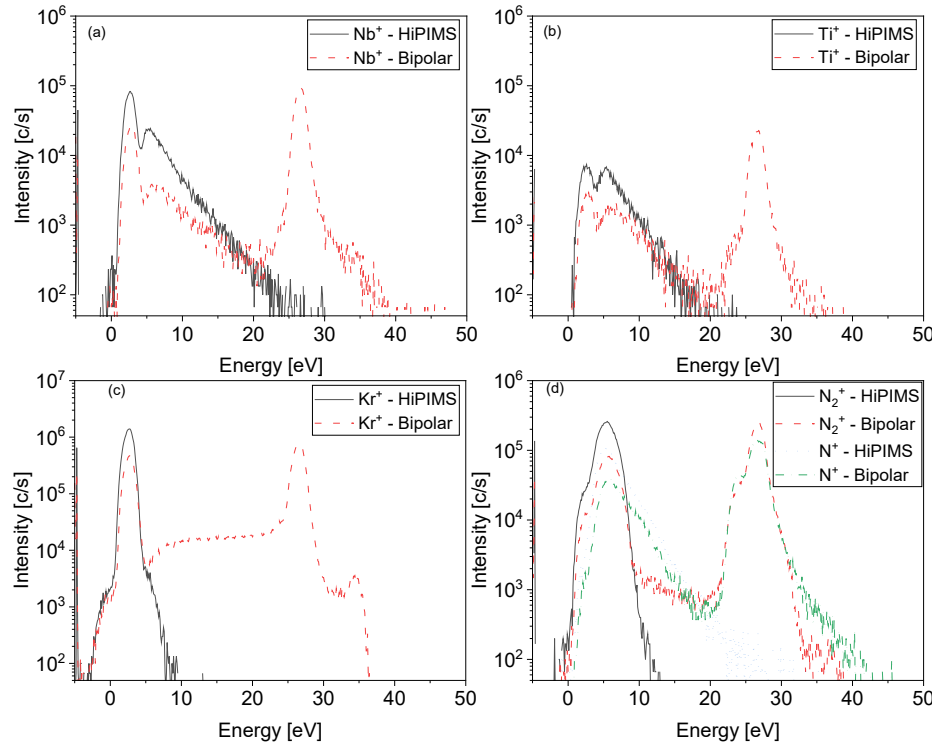


Figure 4: IEDF of  $\text{Nb}^+$  (a),  $\text{Ti}^+$  (b),  $\text{Kr}^+$  (c),  $\text{N}_2^+$  and  $\text{N}^+$  (d) obtained for HiPIMS and bipolar HiPIMS at  $1 \times 10^{-2}$  mbar.

by the reverse potential and gained the same energy per unit charge. The Kr ions however are found outside the magnetic trap and gained only a portion of the acceleration.

IEDF of nitrogen ions show similar trend as reported from the Kr positive ions. However, the fall observed in the  $\text{Kr}^+$  case does not happen for the  $\text{N}_2^+$  and  $\text{N}^+$ . As nitrogen is part of the gas mixture and participate in the deposition on the substrate, its likely that they have similar behaviour as Nb and Ti positive ions. As reported in [13], the behaviour of the ions will depend on their location at the end of the negative pulse; furthermore, an increase of  $U_{rev}$  or modification of the positive pulse width will also have an impact on the ion energies. These properties of the bipolar HiPIMS appear to be promising to promote film adhesion and growth onto substrate.

## CONCLUSION

In this work, both classic and bipolar HiPIMS were investigated for the production of Nb and NbTiN thin films. From the mass scan we can observe the ions of interest and how the addition of nitrogen can influence their formation, the mass scan also helps in preparing the IEDF analysis. From the IEDF, the use of bipolar HiPIMS has a positive impact on the energy intensity of the sputtered ions and could help in improving their production. This can

explain the improvement observed for in enhancing thin film growth compared to other techniques such as DCMS.

## FUTURE WORK

Several aspects of bipolar HiPIMS are still unsolved and need further investigation. The combination of different plasma diagnostics could help in resolving these such as the use of retarding field analyser and/or Langmuir probe, by comparing the results obtained using mass spectrometry. Finally, the production of NbTiN films is currently investigated and analysed using SEM, SIMS and XPS. This will help to link the gas phase process to the film surfacique structure. These topics are currently investigated at Daresbury Laboratories and the University of Liverpool.

## REFERENCES

- [1] A. Gurevich, "Enhancement of rf breakdown field of superconductors by multilayer coating," *Applied Physics Letters*, vol. 88, no. 1, 2006.
- [2] R. Valizadeh *et al.*, "Synthesis of Nb and Alternative Superconducting Film to Nb for SRF Cavity as Single Layer," in *Proc. SRF'21*, East Lansing, MI, USA, 2022, p. 893. doi:10.18429/JACoW-SRF2021-FROFDV06
- [3] C. James *et al.*, "Superconducting nb thin films on cu for applications in srf accelerators," *IEEE transactions on applied superconductivity*, vol. 23, no. 3, pp. 3 500 205–3 500 205, 2012.

- [4] R. Di Leo, A. Nigro, G. Nobile, and R. Vaglio, "Nbodium-titanium nitride thin films for superconducting rf accelerator cavities," *Journal of Low Temperature Physics*, vol. 78, pp. 41–50, 1990.
- [5] A. Miyazaki and W. V. Delsolaro, "Two different origins of the q-slope problem in superconducting niobium film cavities for a heavy ion accelerator at cern," *Physical Review Accelerators and Beams*, vol. 22, no. 7, p. 073 101, 2019.
- [6] J. Vyskočil and J. Musil, "Cathodic arc evaporation in thin film technology," *Journal of Vacuum Science & Technology A: Vacuum, Surfaces, and Films*, vol. 10, no. 4, pp. 1740–1748, 1992.
- [7] G. Greczynski, I. Zhirkov, I. Petrov, J. E. Greene, and J. Rosén, "Control of the metal/gas ion ratio incident at the substrate plane during high-power impulse magnetron sputtering of transition metals in ar," *Thin Solid Films*, vol. 642, pp. 36–40, 2017.
- [8] U. Helmersson, M. Lattemann, J. Bohlmark, A. P. Ehiasarian, and J. T. Gudmundsson, "Ionized physical vapor deposition (ipvd): A review of technology and applications," *Thin solid films*, vol. 513, no. 1-2, pp. 1–24, 2006.
- [9] I.-L. Velicu *et al.*, "Energy-enhanced deposition of copper thin films by bipolar high power impulse magnetron sputtering," *Surface and Coatings Technology*, vol. 359, pp. 97–107, 2019.
- [10] B. Wu *et al.*, "Cu films prepared by bipolar pulsed high power impulse magnetron sputtering," *Vacuum*, vol. 150, pp. 216–221, 2018.
- [11] G. Terenziani, S. Calatroni, and A. Ehiasarian, "Nb coatings for superconducting rf applications by hipims," *CERN, Geneva*, 2013.
- [12] M. Mišina, L. R. Shaginyan, M. Maček, and P. Panjan, "Energy resolved ion mass spectroscopy of the plasma during reactive magnetron sputtering," *Surface and Coatings Technology*, vol. 142, pp. 348–354, 2001.
- [13] J. Keraudy, R. P. B. Viloan, M. A. Raadu, N. Brenning, D. Lundin, and U. Helmersson, "Bipolar hipims for tailoring ion energies in thin film deposition," *Surface and Coatings Technology*, vol. 359, pp. 433–437, 2019.